Brain Pathology ISSN 1015-6305

RESEARCH ARTICLE

Mitochondrial ATP-Synthase in the Entorhinal Cortex Is a Target of Oxidative Stress at Stages I/II of Alzheimer's Disease Pathology

Beatrice Terni[1]; Jordi Boada[2]; Manuel Portero-Otin[2]; Reinald Pamplona[2]; Isidro Ferrer[1]

[1] Institut de Neuropatologia, Servei Anatomia Patològica, IDIBELL, Hospital Universitari de Bellvitge, Universitat de Barcelona, CIBERNED, Hospitalet de Llobregat, Barcelona, Spain.
[2] Department of Experimental Medicine, University of Lleida-IRBLLEIDA, 25008 Lleida, Spain.

Keywords
Alzheimer disease stage I/II, ATP-synthase α chain, entorhinal cortex, lipid peroxidation, oxidative stress.

Corresponding author:
Isidro Ferrer, Prof, Institut de Neuropatologia, Servei Anatomia Patològica, Hospital Universitari de Bellvitge, Care Feixa LLarga sn, 08907 Hospital et de Llobregat, Spain (E-mail: *8082ifa@comb.es*)

Received 15 October 2008; revised 15 October 2008; accepted 21 November 2008.

doi:10.1111/j.1750-3639.2009.00266.x

Abstract

Oxidative stress has been implicated in the pathogenesis of several neurodegenerative diseases including Alzheimer's disease (AD). Several proteins have been identified as targets of oxidative damage in AD dementia (usually stages V/VI of Braak) and in subjects with mild cognitive impairment associated with middle stages of AD pathology (stage IV of Braak). In this study, we investigate whether brain proteins are locally modified by oxidative stress at the first stages of AD-related pathology when morphological lesions are restricted to the entorhinal and transentorhinal cortices of neurofibrillary pathology (stages I/II of Braak). Using a proteomic approach, we show that the α subunit of the mitochondrial adenosine triphosphate (ATP)-synthase is distinctly lipoxidized in the entorhinal cortex at Braak stages I/II compared with age-matched controls. In addition, ATP-synthase activity is significantly lower in Braak stages I/II than age-matched control, while electron transport chain, expressed by the mitochondrial complex I activity, remains not affected. This is the first study showing oxidative damage in the first stage, and clinically silent period, of AD-related pathology characterized by entorhinal and transentorhinal tauopathy.

INTRODUCTION

Alzheimer's disease (AD) is a common neurodegenerative disease characterized by senile plaques (SPs), neurofibrillary tangles (NFTs), synaptic dysfunction and neuronal deficits. Recent studies have indicated that the pathogenesis of AD is a complex and heterogeneous process; in addition to NFTs and SP, gliosis, chronic inflammatory reactions and oxidative stress contribute to the progression of the disease (10, 11, 19, 55).

All aerobic organisms produce certain levels of reactive oxygen species (ROS), mostly generated during cellular respiration in mitochondria. However, oxidative stress becomes harmful when the production of ROS exceeds the cellular antioxidant capacity. Oxidative damage occurs at the level of DNA, RNA, lipids, sugars and proteins, and it appears to be a very important factor in the pathogenesis of AD. High levels of redox-active iron and copper, which have a role in free-radical production, are found in NFTs and Aβ plaques (28, 45). In addition, several studies have shown an increase of oxidative damage in AD brains and in the cerebrospinal fluid of patients affected by the disease (24, 32, 35, 46). Oxidative modification of proteins can occur as direct oxidation of the protein side-chain by ROS, which results in the formation of hydroxyl groups or carbonyl groups. On the other hand, products of glycoxidation and lipoxidation can form stable adducts with aminoacids, leading to structural alterations of proteins (9, 43). Protein oxidation results in altered biologic function and leads to abnormal protein cross-linking and aggregation; these two events can lead to cell degeneration (31, 48).

Increased levels of glycation end products and lipid peroxidation markers have been observed in brains of patients with AD in association with NFTs and Aβ deposits (23, 47, 56). One of the main products of lipoxidation is 4-hydroxy-2-nonenal (HNE), a highly reactive aldehyde that can form stable adducts with cysteine, histidine and lysine (53). Several studies have shown that HNE is neurotoxic and can inhibit enzymes essential for neuronal survival such as the Na^+/K^+ ATPase (18, 31).

Many studies have identified targets of oxidative stress in advanced stages of AD (6, 21, 37, 50). Mild cognitive impairment is a heterogeneous condition generally characterized by memory disturbances (29). Neuropathologically, a substantial number of patients with mild cognitive impairment are associated with AD pathology in the entorhinal and transentorhinal cortices, amygdala, hippocampus and temporal lobe (42). Increased levels of HNE are also present in the brains of subjects with mild cognitive impairment and early AD (8, 54). Protein oxidative damage has also been shown in patients with mild cognitive impairment associated with AD pathology (7, 20, 52, 54). Oxidative damage is not restricted to proteins, but DNA and RNA are also targets of oxidation in cases

Table 1. Summary of neuropathological findings in this series. Abbreviations: AD = Alzheimer's disease; NFTs = neurofibrillary tangles; NP = neuritic plaques; DP = diffuse plaques; AA = amyloid angiopathy.

AD cases	Age	Gender	Post-mortem	NFTs: tau pathology	Amyloid pathology
Cases					
1	67	Male	7h15–	AD II	No
2	82	Female	5h15–	AD I	DP, AA
3	69	Male	4h15–	AD II	No
4	72	Male	6h15–	AD II	DP, NP
5	55	Male	3h10	AD I	No
6	53	Male	6h15–	AD I	DP
Controls					
1	73	Female	5h30	No	No
2	80	Female	3h30	No	No
3	65	Female	4h	No	No
4	73	Female	7h	No	No
5	59	Male	6h25	No	No
6	53	Male	7h25	No	No

with mild cognitive impairment (25, 26). Together, these observations support previous proposals suggesting oxidative damage as an early event in AD (36).

Mild cognitive impairment can be the initial clinical manifestation of AD (39). However, AD pathology associated with mild cognitive impairment is certainly not the less severe neuropathological expression of AD-related pathology. Braak *et al* proposed a classification of AD in six stages according to the severity and regional distribution of NFT pathology (5). Stages I/II are characterized by NFTs and dystrophic neurites restricted to the transentorhinal and entorhinal cortices. No clinical symptoms are noted at these stages. Stages III/IV are characterized by the additional involvement of the hippocampus and inner regions of the temporal cortex. Mild cognitive impairment may occur in association with AD Braak stages III/IV. Finally, stages V/VI involve the neocortex and are clinically manifested as Alzheimer dementia.

It is not known whether oxidative damage occurs at Braak stages I/II in which NFT pathology is restricted to the entorhinal and transentorhinal cortices. Yet this appears to be a substantial piece of information as it would permit to know at what point of AD oxidative does damage initiate and can be detected. To reach this end, the present study was designed to examine oxidative damage in the entorhinal cortex, the first brain region to be affected by NFT in AD-related pathology. We show that the mitochondrial ATP-synthase α subunit is lipoxidized in the entorhinal cortex in Braak stages I/II and that there is a specific loss of enzymatic activity, indicating that an alteration of the energy production system may be one of the first pathways to be impaired at the initial stages of AD-related tauopathy.

MATERIALS AND METHODS

Tissue samples

The selection of cases examined in the present study corresponded to a consecutive series of donations having in common (i) lack of neurological symptoms and signs; (ii) lack of known hepatic or renal function impairment; and (iii) lack of evidence of prolonged agonal state. At autopsy, half of each brain was fixed in formalin, while the other half was cut in coronal sections 1 cm thick, frozen on dry ice and stored at −80°C until use. For diagnostic morphological studies, the brains were fixed by immersion in 4% buffered formalin for 2 or 3 weeks. The neuropathological study was carried out on sections of the frontal (area 8), primary motor, primary sensory, parietal, temporal superior, temporal inferior, anterior cingular, anterior insular, and primary and associative visual cortices; entorhinal cortex and hippocampus; caudate, putamen and pallidum; medial and posterior thalamus; subthalamus; Meynert nucleus; amygdala; midbrain (two levels), pons and medulla oblongata; and cerebellar cortex and dentate nucleus. The tissue was embedded in paraffin. De-waxed sections, 5 μm thick, were stained with hematoxylin and eosin, and with Klüver-Barrera, or processed for immunohistochemistry according to the streptavidin LSAB method (Dako, Dakopats, Barcelona, Spain). After incubation with methanol and normal serum, the sections were incubated with one of the primary antibodies at 4°C overnight. Antibodies to glial fibrillary acidic protein (GFAP, Dako), βA4-amyloid (Boehringer, Ingelheim, Germany) and ubiquitin (Dako) were used at dilutions of 1:250, 1:50 and 1:200, respectively. Antibodies to α-synuclein (Dako) were used at a dilution of 1:100. Phospho-specific tau rabbit polyclonal antibodies Thr181, Ser199, Ser202, Ser214, Ser231, Ser262, Ser396 and Ser422 (all of them from Calbiochem, LaJolla, CA, USA) were used at a dilution of 1:100, excepting anti-phospho-tauThr181, which was used at a dilution of 1:250. The peroxidase reaction was visualized with 0.05% diaminobenzidine and 0.01% hydrogen peroxide. Staging of AD was carried out according to Braak criteria (5), adapted to paraffin sections (4).

Cases with no neuropathological lesions (including vascular, hypoxic, inflammatory and degenerative) were considered as controls. Cases with NFT restricted to the entorhinal and transentorhinal cortices, with and without moderate amyloid burden, were included in the present study. Cases with additional pathology (either tau (ie, grains), α-synuclein, Lewy bodies in other brain regions, or vascular in any area) were excluded. Moreover, GFAP immunohistochemistry was used to discard astrocytosis in any case. The clinical records were reexamined for every case, and cases with AD-related pathology were reassessed by phone calls or interviews to their relatives, asking for any, even subtle, neurological or cognitive change. Only cases fulfilling these criteria were considered in the present work.

A summary of the cases analyzed is shown in Table 1. Age, gender, post-mortem delay and neuropathological diagnosis are reported for cases with early AD pathology and control individuals.

Sample preparation

An amount of 0.1 g of entorhinal cortex from the six cases with AD pathology stages I/II and six controls was homogenized with a glass homogenizer in buffer containing 8 M Urea, 2 M Thiourea, 50 mM Tris-HCl pH 7.5, 4% CHAPS, 1 mM phenylmethylsulfonyl fluoride (PMSF) plus protease inhibitors tablet (Roche Molecular Systems, Barcelona, Spain) and then centrifuged for 10 minutes at 10 000 *g*. After centrifugation, the supernatant was conserved, and the total amount of protein was quantitated by using the Comassie brilliant blue-based Bradford assay (Sigma-Aldrich, Madrid, Spain). For two-dimensional (2-D) electrophoresis, 2% biolytes 3/10 ampholytes (BioRad, Barcelona, Spain), 4 mM of Tributylphosphine and Bromophenol blue were added to the samples.

For the study of mitochondrial-enriched fractions, the following procedure was applied: 0.2 g of tissue from three AD cases and three controls was homogenized and sonicated on ice in 1.5 mL of buffer containing 20 mM HEPES pH 7.5, 250 mM sucrose, 10 mM KCl, 1.5 mM $MgCl_2$, 1 mM EDTA, 1 mM EGTA, 1 mM dithiotreitol (DTT), 1 mM PMSF plus protease inhibitors cocktail (Roche) and then was centrifuged for 30 minutes at 750 *g*. The pellet (P1) was discarded, while the supernatant was centrifugated for 20 minutes at 8000 *g*. The pellet (P2), corresponding to the mitochondrial-enriched fraction, was resuspended in buffer with 8 M Urea, 2 M Thiourea, 50 mMTris pH 7.5, 4% CHAPS. For protein quantitation, Bradford assay was used. Immediately before the 2-D-electrophoresis run, 2% biolytes 3/10 ampholyites (BioRad), 4 mM of Tributylphosphine and Bromophenol blue were added to the samples.

2-D gel electrophoresis

For the first dimension electrophoresis, 200 μg of protein from the six cases with AD pathology stages I/II and six controls was applied onto 7 cm pH 3–10 nonlinear gradient ReadyStrip IPG strips (BioRad) that were actively rehydrated at 50 V for 12 h. The isoelectric focusing was performed rapidly at 200 V for 1 h, linearly at 500 V for 1 h, linearly at 1000 V for 1 h, linearly at 8000 V for 1 h and rapidly at 8 000 V for 10 h. All the above steps were carried out at room temperature. After focusing, the strips were kept at −80°C until two-dimensional electrophoresis was performed.

For the second-dimension electrophoresis, the strips were first equilibrated for 10 minutes in a buffer containing 375 mM Tris-HCl pH 8.8, 6 M urea, 2% (w/v) sodium dodecyl sulfate (SDS), 20% (v/v) glycerol, and 2% DTT, and then reequilibrated for another 10 minutes in the same buffer in which DTT was replaced by 2.5% iodoacetamide. Proteins were separated by SDS-polyacrylamide gel (PAGE) using 10% polyacrylamide gels, and the precision protein marker (Fermentas, Glen Burnie, MD, USA) was run along with the sample at 100 V for 2 h. Two gels of the same sample were run in parallel. One gel was stained with Bio-Safe colloidal Comassie Brilliant Blue G-250 (BioRad) according to the manufacturer's guidelines, and the other one was processed for Western blot analysis.

Western blotting

For immunoblotting analysis, proteins were transferred to a nitrocellulose membrane (BioRad) at 100 V for 75 minutes, after SDS-PAGE electrophoresis. Once the transfer was completed, membranes were treated with 10 mM $NaBH_4$ in Tris-buffer saline (TBS) for 30 minutes in order to stabilize the HNE-protein adducts, and washed three times with TBS. Afterward, the membranes were blocked with 5% skimmed milk for 1 h and immunoblotted overnight a 4°C with polyclonal anti-HNE antibody (Calbiochem) or with monoclonal anti-ATP-synthase α chain antibody (Bioscience, Barcelona, Spain). Blots were then incubated with anti-rabbit/mouse secondary antibody horseradish peroxidase conjugated (Dako) and visualized with the ECL chemiluminescence method (Amersham, Barcelona, Spain). The monoclonal anti-β-actin antibody (Sigma-Aldrich) was used at a dilution of 1:5000 as a control of protein loading normalization in monodimensional gels.

Protein expression levels were determined by densitometry of the bands by using Total Laboratory v2.01 software (Nonlinear Dynamics Ltd., Newcastle upon Tyne, UK). Measurements are expressed as arbitrary units. The results were normalized for β-actin. The numerical data obtained from AD cases and corresponding controls were statistically analyzed with STATGRAPHICS plus 5.0 software (Madrid, Spain) and by using the analysis of variance (ANOVA) test.

Afterward, both strips were incubated with anti-HNE antibody at 1:1000 dilution and then with antirabbit secondary antibody horseradish peroxidase conjugated (Dako) and visualized with the ECL chemiluminescence method.

$NaBH_4$ treatment

Entorhinal cortex of one AD I/II case was homogenized in lysis buffer containing 8 M Urea, 2 M Thiourea, 50 mM Tris-HCl pH 7.5, 4% CHAPS, 1 mM phenylmethylsulfonyl fluoride (PMSF) plus protease inhibitors tablet (Roche Molecular Systems, Barcelona, Spain) and then centrifuged for 10 minutes at 10 000 g. After centrifugation, the total amount of protein of the supernatant was quantitated by using the Coomassie brilliant blue-based Bradford assay (Sigma-Aldrich). An amount of 30 μg of protein from the same AD I/II homogenate was loaded respectively in two separate lanes of an SDS-PAGE and then blotted into a nitrocellulose membrane. The membrane was cut between the two lanes, and one part was treated with 10 mM $NaBH_4$ for 30 minutes, while the other one was not.

In-gel digestion

Proteins were in-gel digested with trypsin (Promega, Barcelona, Spain) in the automatic Investigator ProGest robot of Genomic Solutions, MI, USA. Briefly, excised gel spots were washed sequentially with ammonium bicarbonate buffer and acetonitrile. Proteins were reduced with 10 mM DTT solution for 30 minutes and alkylated with 100 mM solution of iodine acetamide. After sequential washings with buffer and acetonitrile, proteins were digested overnight at 37°C with trypsin 0.27 nM. Tryptic peptides were extracted from the gel matrix with 10% formic acid and acetonitrile. The extracts were pooled and dried in a vacuum centrifuge.

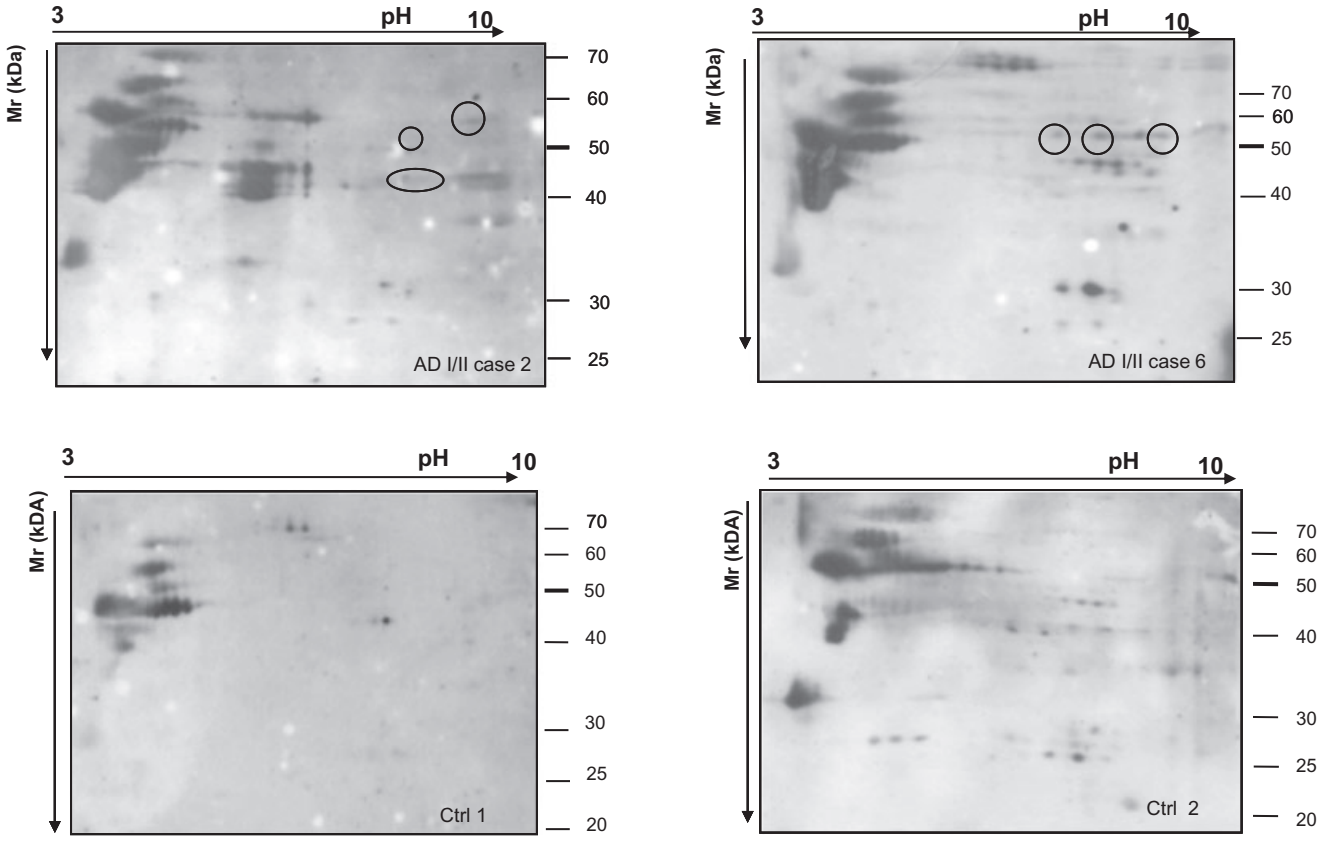

Figure 1. 2-D gels immunoblotted with HNE antibody of entorhinal cortex from AD cases stages I/II (cases 2 and 6, upper panel) and controls (Ctrl 1 and 2, lower panel). Spots positive for HNE antibodies detected in AD but not in control cases are encircled. Note that several other spots appeared in case 2 but not in case 6. Similarly, additional spots appeared in Ctrl 2 but not in Ctrl 1. That means that other proteins in control and diseased brains are subject of oxidation. Only the spots appearing in all AD stage I/II cases and in none control were analyzed in detail. Abbreviations: 2-D = two-dimensional; AD = Alzheimer's disease.

Acquisition of MS and mass spectrometry (MS/MS) spectra

Proteins excised from the 2-D gels were either analyzed by matrix assisted laser desorption ionization-time-of-flight (MALDI-TOF/TOF) (4700 Proteomics Analyzer, Applied Biosystems, Foster city, CA, USA) or electrospray ionization-q-time-of-flight (ESI-Q-TOF) (Qtof-Global, Micromass-Waters, Manchester, UK). In the first case, the digests were redissolved in 5 µL of 0.1% trifluoroacetic acid. Typically, a 0.5 µL aliquot was mixed with the same volume of a matrix solution, 5 mg/mL of α-ciano-4-hydroxycinnamic acid (Sigma-Aldrich) in 50% acetonitrile/0.1% trifluoroacetic acid. A maximum of five prominent peaks was selected to be characterized further by MS/MS analysis. Spectra were submitted for database searching in a generic MASCOT (Matrix Science, Boston, MA, USA) format.

Some of the tryptic digested samples were analyzed by online liquid chromatography tandem mass spectrometry (Cap-LC-nano-ESI-Q-TOF) (CapLC, Micromass-Waters, Manchester, UK). In that case, samples were resuspended in 12 µL of 10% formic acid solution, and 4 µL was injected to chromatographic separation in reverse-phase capillary C_{18} column (75 µm of internal diameter and 15 cm length, PepMap column, LC Packings, Amsterdam, the Netherlands). The eluted peptides were ionized via coated nano-ES needles (PicoTip™, New Objective, Woburn, MA, USA). A capillary voltage of 1800–2200 V was applied together with a cone voltage of 80 V. The collision in the collision-induced dissociation (CID) was 20–35 eV and argon was used as collision gas. Data were generated in PKL file format, which were submitted for database searching in MASCOT server.

Probability-based MOWSE score was used to determine the level of confidence in the identification of specific isoforms from the mass spectra. This probability equals $10^{(-\text{Mowse score}/10)}$. Mowse scores greater than 50 were considered to be of high confidence of identification.

Measurement of the mitochondrial complex I and complex V activities

For mitochondrial complex I, entorhinal tissue homogenates were centrifuged at 70 000 *g* for 30 minutes at 4°C. The resulting membranous pellets were resuspended and sonicated in ice-cold potassium phosphate buffer (pH 7.4) in order to obtain inverted submitochondrial particles. The rate of NADH oxidation in the resultant suspensions was measured spectrophotometrically at 340 nM and 37°C in a medium containing 0.3 mM NADH, 0.1 mM coenzyme Q1, 1 mM potassium cyanide and 2 mM sodium azide, in the presence and absence of 1 µM rotenone. Complex I-specific enzyme

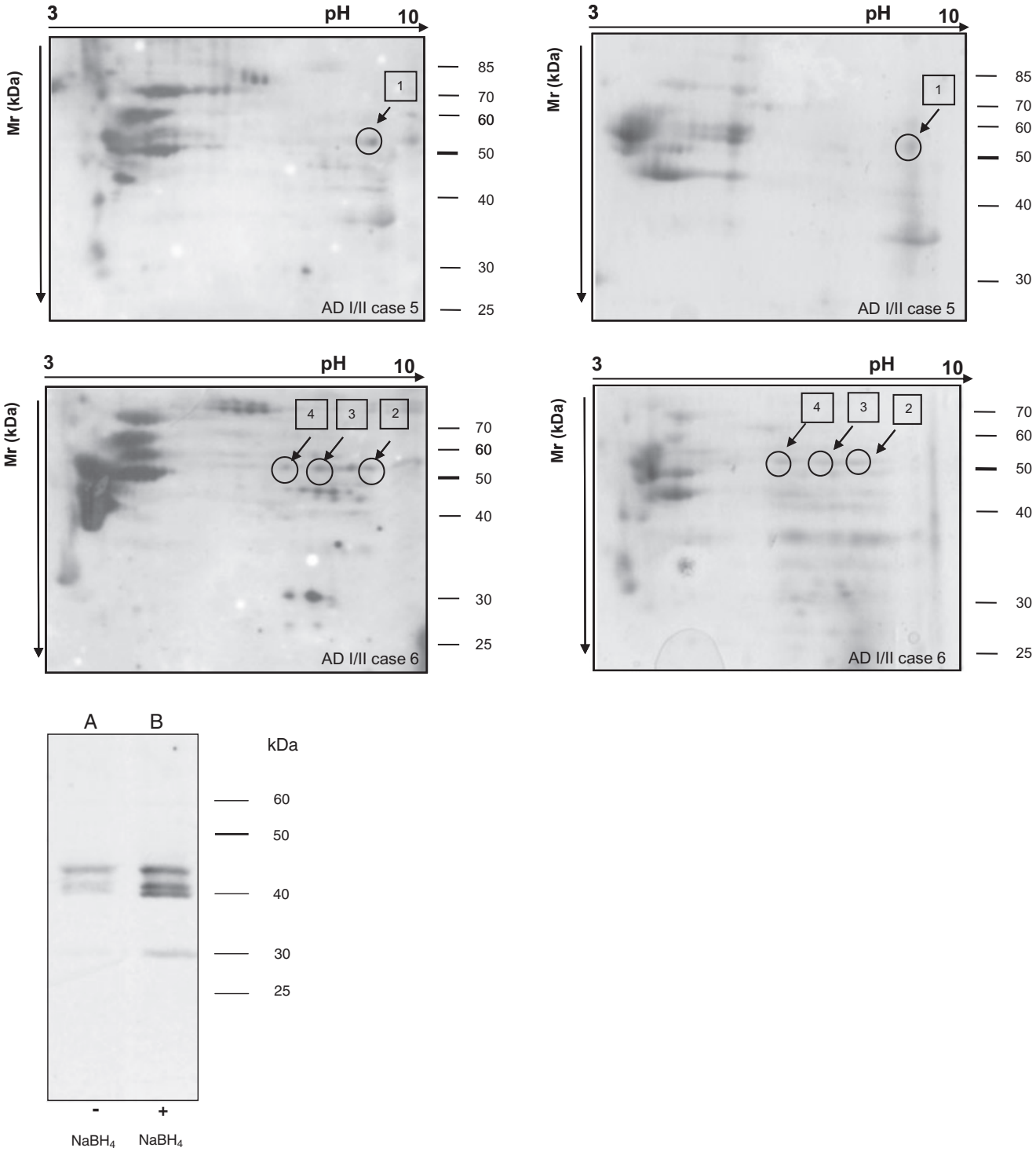

Figure 2. 2-D gel electrophoresis and Western blotting to HNE (left panel) processed in parallel with gels stained with Comassie (right panel). HNE-immunoreactive spots in blotted membranes of AD stages I/II cases 5 and 6 are identified in gels stained with Comassie. The spots #1 from case 5 and spots #2, #3 and #4 from case 6 were in-gel digested and processed for mass spectrometry. Target protein is shown in Table 2. (Inset) Homogenates were loaded respectively in two separate lanes of an SDS-PAGE and then blotted into a nitrocellulose membrane. The membrane was cut between the two lanes and one part was treated with 10 mM $NaBH_4$, while the other one was not. $NaBH_4$-treated membrane strip (lane B) shows a much more intense signal than the strip that was not treated with the reducing agent (lane A). Abbreviations: 2-D = two-dimensional; HNE = 4-hydroxy-2-nonenal; AD = Alzheimer's disease; SDS-PAGE = sodium dodecyl sulfate polyacrylamide gel.

Table 2. Mass spectrometry protein identification of the HNE-positive spots of AD I/II entorhinal cortex. HNE positive spots from all the AD cases were analyzed: spot #1 from AD case 5; spots #2, 3 and 4 from AD case 6; spot #5 from AD case 4, spots #6 and 7 from AD case 1; spot #8 from AD case 2; and spots #9 and 10 from AD case 3. Abbreviations: HNE = 4-hydroxy-2-nonenal; AD = Alzheimer's disease; ATP = adenosine diphosphate.

Spot	Protein	Theorical PI	Theorical MW	Sequence coverage	MOWSE score
1	**gil127798841** ATP-synthase, H + transporting mitochondrial F1 complex, α subunit	9.07	59785	33%	236*
2	**gil34782901** ATP-synthase, H + transporting mitochondrial F1 complex, α subunit	9.10	48879	21%	90*
3	**gil34782901** ATP-synthase, H + transporting mitochondrial F1 complex, α subunit	9.10	48879	18%	102*
4	**gil34782901** ATP-synthase, H + transporting mitochondrial F1 complex, α subunit	9.07	48879	18%	162*
5	**gil4757810** ATP-synthase, H + transporting mitochondrial F1 complex, α subunit	9.16	59828	25%	445§
6	**gil4757810** ATP-synthase, H + transporting mitochondrial F1 complex, α subunit	9.16	59828	28%	627§
7	**gil127798841** ATP-synthase, H + transporting mitochondrial F1 complex, α subunit	9.07	59785	16%	320§
8	**gil4757810** ATP-synthase, H + transporting mitochondrial F1 complex, α subunit	9.14	59828	27%	616§
9	**gil127798841** ATP-synthase, H + transporting mitochondrial F1 complex, α subunit	9.07	59785	27%	152*
10	**gil4757810** ATP-synthase, H + transporting mitochondrial F1 complex, α subunit	9.16	59828	42%	980§

All the spots correspond to the mitochondrial ATP-synthase α subunit.
Score values higher than 50 indicate identity or extensive homology ($P < 0.05$).
*MALDI-TOF/TOF used for the analysis.
§ESI-Q-TOF used for the analysis.

activity was calculated as the rotenone-sensitive rate and expressed in units/mg of protein. One unit of complex I oxidizes 1 μmol of NADH per minute (16, 34).

Complex V enzyme activity was measured in entorhinal homogenates with a MitoProfile® Rapid Microplate Assay Kit for ATP-synthase (complex V) (Mitosciences, OR, USA) according to the manufacturer's instructions. This method is based on specificity of clones 12F4AD8 (recognizing native F1 portion) and 3D5AB1 (recognizing ß subunit) for complex V immunoisolation. Briefly, the ATP-synthase enzyme was immunocaptured within the wells of the microplates, and the enzyme activity was measured by monitoring the decrease in absorbance at 340 nM. Specifically, the conversion of ATP to ADP by ATP-synthase was coupled to the oxidation reaction of nicotinic acid adenine dinucleotide (NAD+) to reduced nicotinamide adenine dinucleotide (NADH) with a reduction in absorbance at 340 nM. Additional experiments, using the ATP reverse hydrolysis on inverted submitochondrial particles (see above) with inorganic phosphate measurement based on malachite green assay (Cayman ref 10009325, Malachite Green Phosphate Assay Kit) showed similar results to immunoisolated complex V activity assay (data not shown).

Complex I- and complex V-specific activities were normalized per protein content and per citrate synthase activity. Citrate synthase activity in a specific tissue is frequently constant when expressed per mitochondrial protein. Some metabolic mitochondrial parameters, therefore, may be expressed per citrate synthase for specific applications (17, 22, 41). The activity of citrate synthase in the tissue homogenate supernatants was measured spectrophotometrically at 412 nM and 30°C in a medium containing 0.1 mM 5,5-dithiobis-(2-nitrobenzoic) acid, 0.5 mM oxaloacetate, 50 μM EDTA, 0.31 mM acetyl coenzyme A, 5 mM triethanolamine hydrochloride and 0.1 M Tris–HCl, pH 8.1 as described previously (44).

Double-labeling immunofluorescence and confocal microscopy

De-waxed 5-micron-thick sections were stained with a saturated solution of Sudan black B (Merck, Barcelona, Spain) for 10 minutes to block the autofluorescence of lipofuscin granules present in nerve cell bodies, rinsed in 70% ethanol and washed in distilled water. The sections were incubated at 4°C overnight with a combination of the primary antibodies to ATP-synthase and phospho-tauThr181. The mouse anti-ATP-synthase antibody (Biosciences) was used at a dilution of 1:1000 and the anti-phospho-tauThr181 antibody (Calbiochem) at a dilution of 1:500. After being washed in phosphate-buffered saline (PBS), the sections were incubated in the dark for 45 minutes at room temperature, with the cocktail of secondary antibodies diluted in the same vehicle solution as the primary antibodies. Secondary antibodies were Alexa488 antimouse and Alexa555 antirabbit (both from Molecular Probes, Invitrogen, Spain, UK), and these were used at a dilution of 1:400. Nuclei were stained with DRAQ 5 (Molecular Probes) diluted 1:2000. Some sections were incubated only with the secondary antibodies. These sections were considered as negative controls. After being washed in PBS, the sections were mounted in Immuno-Fluore Mounting medium (ICN Biomedicals, Barcelona, Spain), sealed and dried overnight. Sections were examined with a Leica TCS-SL confocal microscope (Wetzler, Germany).

RESULTS

Case analysis

Neuropathological examination was carried out in different brain areas of both AD and control cases, and several antibodies were used for diagnostic morphological studies as reported in the Materials and Methods section. Phospho-specific tau antiserum revealed tau inclusions in the entorhinal cortex of AD I/II cases, while no staining for hyper-phosphorylated tau was observed in any control subjects. β-amyloid deposits were present as diffuse plaques and primitive plaques in the entorhinal cortex of 3 of 6 AD stage I/II cases. No amyloid pathology was detected in control cases (Table 1).

2D gel electrophoresis and mass spectrometry protein identification

Total homogenates of entorhinal cortex from AD I/II and control cases were run in monodimensional gels and analyzed by Western blot using anti-HNE antibodies. Discrete differences in protein oxidation levels were seen between cases with AD pathology stages I/II and controls.

To investigate the nature of lipoxidation targets, 2-D gel electrophoresis was used. This approach allowed the separation of proteins according to their charge and molecular weight for subsequent mass-spectroscopy analysis. Total homogenates of entorhinal cortex from AD stages I/II cases (n = 6) and age-matched controls (n = 6) were run in parallel.

In 2-D Western blots, anti-HNE antibody marked several spots in the membrane of both AD and control subjects (Figure 1). Most of these varied from one case to another and were not reproducible among the AD cases, suggesting individual variations. In order to minimize the risk of false positive results, we decided to study just the spots that were only present in cases with AD pathology stages I/II and that were present in all cases. In this way, we identified a row of spots with a molecular weight between 50 and 60 kDa present in *all* cases with AD pathology stages I/II, but in *none* control (Figure 1). To investigate the identity of these spots, mass-spectroscopy analysis was performed in all six AD-related cases. Samples from each individual with AD were run in parallel in 2D gels. One gel was immunoblotted for anti-HNE antibody, while the other one was stained with Comassie blue. HNE-immunopositive spots were identified in the parallel Comassie-stained gel and processed for mass spectrometry. A total of 10 different spots were analyzed. Spot 1 from AD case 5 and spots 2, 3 and 4 from AD case 6 are shown in Figure 2. The specificity of the anti-HNE antibody has been analysed, and results are shown in Figure 2 inset. The HNE-immunoblot of the $NaBH_4$-treated membrane strip (Figure 2 inset, lane B) shows a much more intense signal than the strip that was not treated with the reducing agent (Figure 2 inset, lane A).

The complete list of the spots, excised from the Comassie gels, is reported in Table 2. The 10 spots analyzed corresponded to the α subunit of mitochondrial ATP-synthase with high level of confidence ($P < 0.005$) (Table 2).

2D immunoblotting for protein validation

To further validate the correct identification of the protein, parallel immunoblot analysis was performed. Blots of 2-D gels from all the AD cases probed with anti-HNE antibody were immunostained with ATP-synthase α subunit monoclonal antibody. Western blots revealed the presence of a row of spots with a molecular weight between 50 and 60 kDa, which likely corresponded to different isoforms of the enzyme (Figure 3). Spots detected with anti-HNE antibody (Figure 3A) matched those immunostained with α subunit of ATP-synthase antibodies (Figure 3B). These signals coming from the staining with the two antibodies corresponded to the protein spots excised from the Comassie-stained gel and processed for mass spectrometry (Figure 3C).

The ATP-synthase α subunit is part of the F1 complex of the ATP-synthase enzyme, located at the mitochondrial inner membrane. To further confirm the lipoxidation state of the α subunit of this enzyme in the entorhinal cortex of AD stages I/II, 2-D HNE

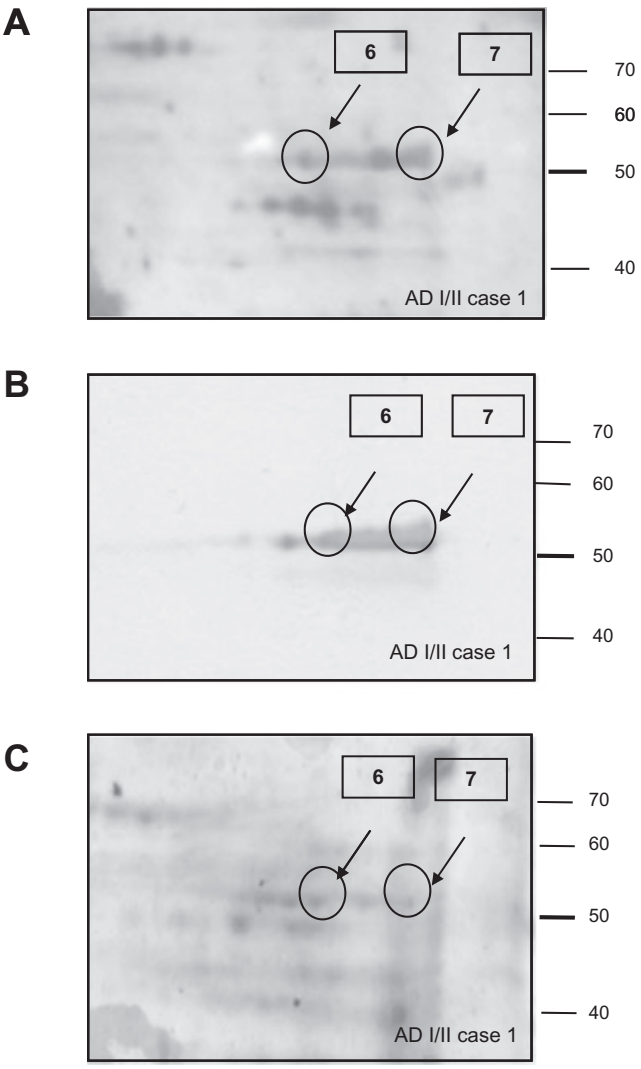

Figure 3. Validation of mass spectrometry results was performed using Western blot analysis. Case 1 is used as an example. **A**. Blot probed with HNE antibody. **B**. Blot probed with ATP-synthase α subunit antibody. **C**. Comassie staining. Proteins analyzed from spots 6 and 7 are listed in Table 2. Abbreviations: HNE = 4-hydroxy-2-nonenal; ATP = ATP-synthase.

immunoblots were performed in mitochondrial-enriched fractions in AD cases. Mitochondrial-enriched fractions were obtained as detailed in Materials and Methods section. Figure 4 shows 2-D immunoblots with anti-HNE and anti-ATP-synthase α subunit antibodies of cases with AD pathology stages I/II (panel A) and controls (panel B). A row of spots, corresponding to α unit of ATP-synthase, was clearly marked with HNE antibody in mitochondrial extracts of diseased cases compared with controls. These data further support the lipoxidation state of the enzyme in mitochondrial fractions.

In order to rule out the possibility that the strong oxidation of the enzyme was a consequence of an increased protein level associated with the AD condition, ATP-synthase α expression levels were tested in total homogenates of cases with AD pathology stages I/II and controls cases. No significant differences were observed

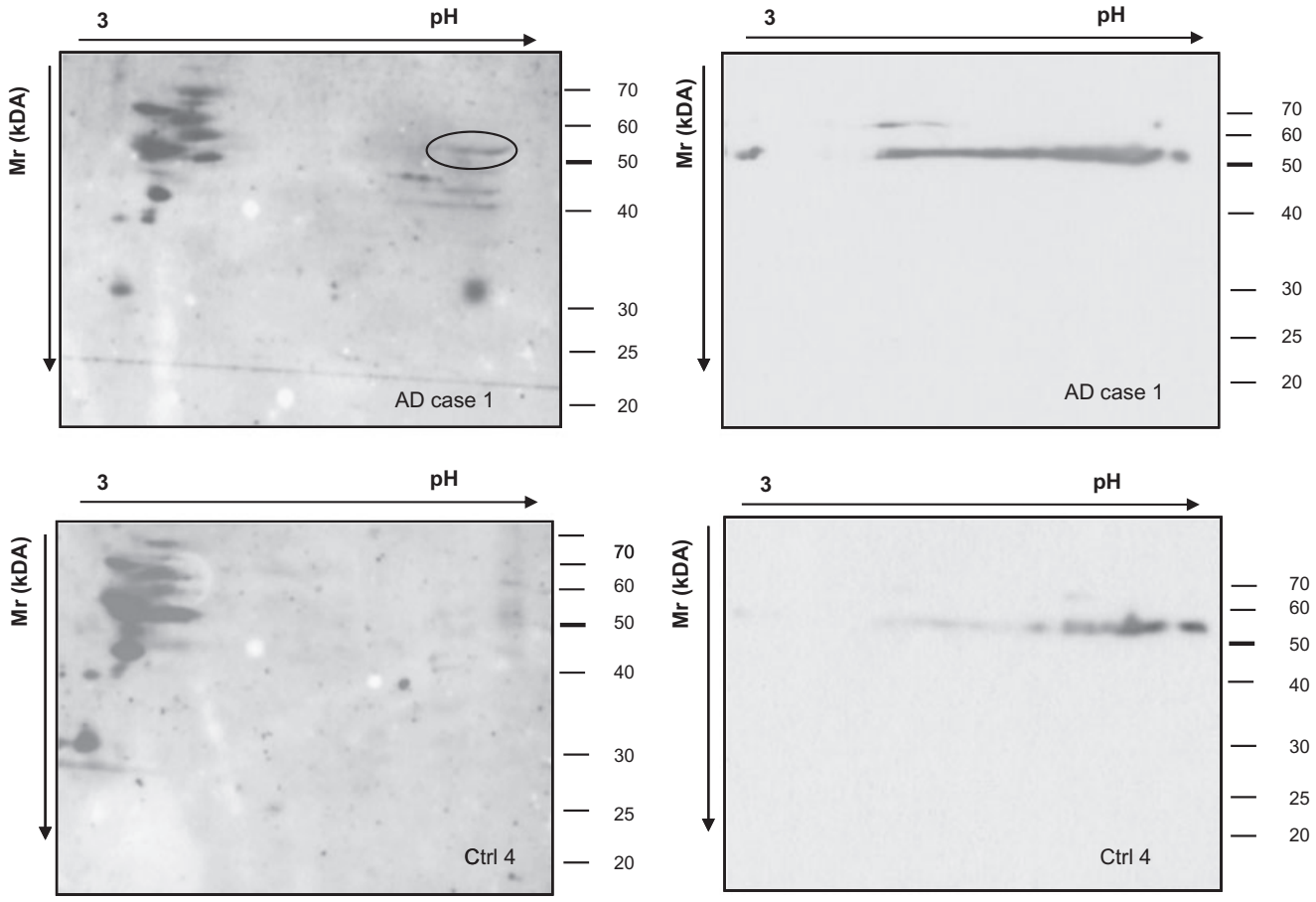

Figure 4. 2-D immunoblots of mitochondrial-enriched fractions of the entorhinal cortex from AD I/II (case 1, upper panel) and control (ctrl 4, lower panel). Immunostaining with anti-HNE (left panels) and anti-ATP-synthase α subunit antibodies(right panel) shows the presence of the lipoxidizedenzyme in AD stage I/II (encircled) but not in control cases. Abbreviations: 2-D = two-dimensional; AD = Alzheimer's disease; HNE = 4-hydroxy-2-nonenal; ATP = ATP-synthase.

between the two groups after densitometric studies normalized with β-actin and statistical processing of data (Student's *t*-test, $P = 0.6$) (Figure 5).

Mitochondrial enzymatic activities

Complex V (ATP-synthase) activity, normalized for citrate synthase activity, was significantly decreased (approximately 30%) in AD Braak stages I/II group (100.0 ± 9.5 vs. 68.8 ± 6.0 for control vs. AD group, mean ± SE, n = 6 per group, respectively; $P = 0.02$) (Figure 5B). No differences between control and AD Braak stages I/II groups were detected for mitochondrial complex I activity (Figure 5B). The complex I activity, also normalized for citrate synthase activity, was 100.0 ± 13.5 vs. 96.0 ± 10.8 for control vs. AD group (mean ± SE, n = 6 per group, $P = 0.41$). Citrate synthase activity was 100.0 ± 13.5 vs. 104.8 ± 8.0 for control vs. AD group (mean ± SE, n = 6 per group; $P = 0.38$).

Double-labeling immunofluorescence and confocal microscopy

Sections immunostained with anti-ATP-synthase and anti-phospho-tau antibodies showed punctate ATP-synthase immunoreactivity consistent with mitochondrial staining in neurons with pretangles, neurons with tangleas and neurons without phospho-tau deposits (Figure 6). Tangles in neurons, but not pretangles, displaced ATPase-immunoreactive dots to the periphery of tangles.

DISCUSSION

Oxidative stress plays an important role in AD, and it has been suggested that oxidative damage is an early event in the pathogenesis of AD (12, 32, 36). There is, indeed, a very important amount of information showing oxidative damage in patients suffering from mild cognitive impairment associated with AD-related pathology consistent with stages III/IV of Braak (5). Oxidative damage targets on proteins, DNA and RNA (7, 8, 20, 25, 26, 30, 37, 40, 52, 54).

However, nothing is known about possible oxidative damage at earlier stages of AD-related pathology, albeit we can understand that this information is really important to know what may occur to the human brain at the very early stages of AD. Therefore, the present study was undertaken to know whether oxidative damage is present even at earlier stages of AD-related pathology, namely, stages I/II of Braak in which NFT pathology is restricted to the entorhinal and transentorhinal cortices. Combination of monodi-

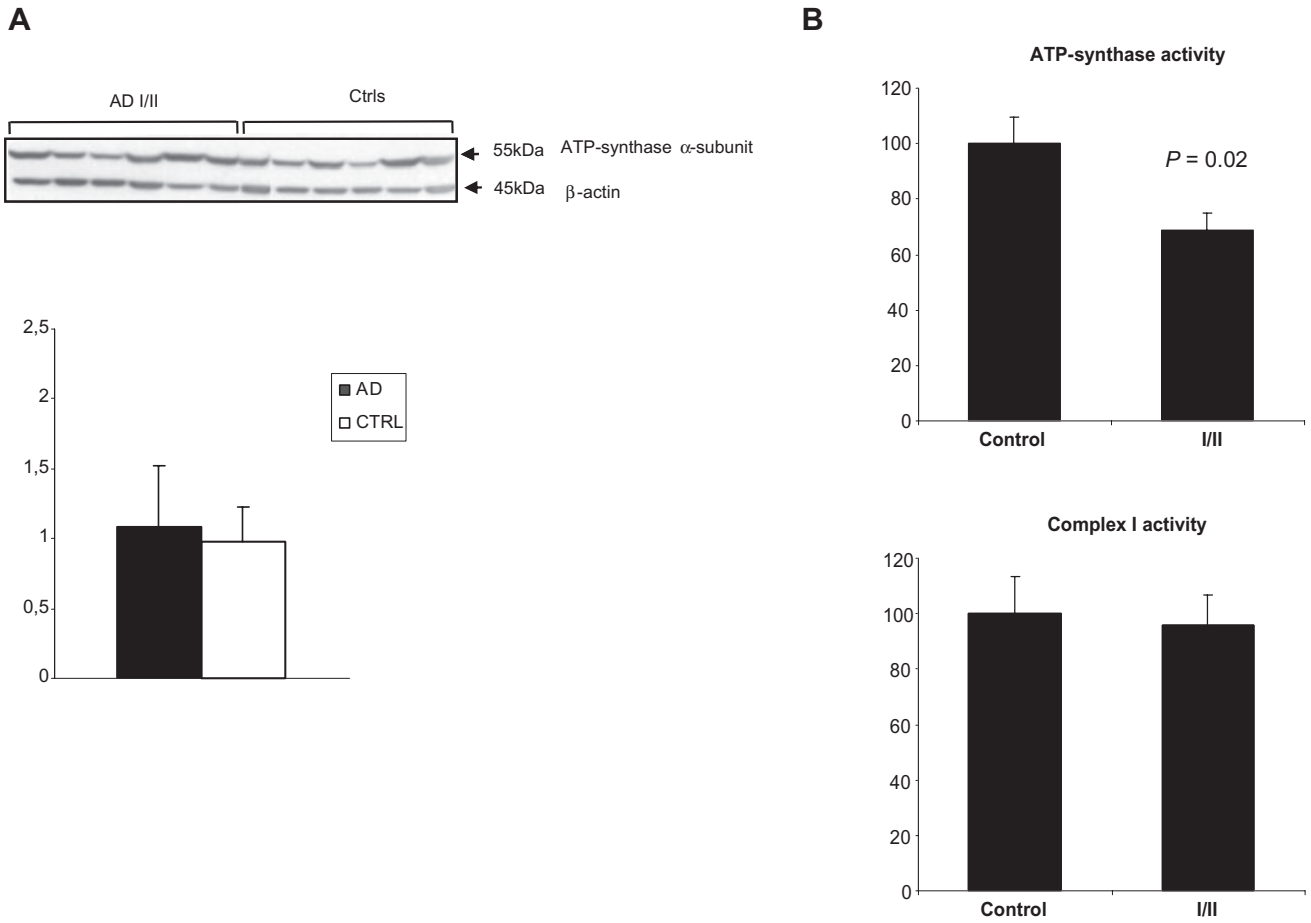

Figure 5. A. Western blots of total entorhinal cortex homogenates in AD cases stages I/II and controls incubated with antibodies to ATP-synthase α subunit. Antibodies to actin were used as a control of protein loading. No significant differences in the expression levels were seen between the two groups (Student's *t*-test, $P = 0.6$). **B.** Complex V (ATP-synthase) activity (% respect control group), normalized for citrate synthase activity, was significantly decreased in AD Braak stages I/II group ($P = 0.02$). No differences between control and AD Braak stages I/II groups were detected for mitochondrial complex I activity ($P = 0.41$). Abbreviations: AD = Alzheimer's disease; ATP = ATP-synthase.

mensional and 2-D gel electrophoresis and Western blotting, in-gel digestion and mass spectrometry, and enzymatic activities was used for this purpose. Although several spots representing lipoxidized proteins were differentially found in individual cases, only those spots that were present in *all* cases with AD pathology stages I/II and in *none* control case were analyzed. The entorhinal cortex was precisely selected because NFT pathology is the main target of NFT pathology at this stage.

The α subunit of the mitochondrial ATP-synthase was recognized as the common lipoxidized protein in the entorhinal cortex of all AD cases at stages I/II.

Mitochondrial ATP-synthase is a multidomain enzyme located in the inner mitochondrial membrane and is the last complex (complex V) of the electron transport chain. It uses the electron proton gradient generated by the electron transport chain to convert ADP molecules to high energy ATP. This enzyme is a large multiprotein complex formed by a transmembrane channel (the F0 complex) and the synthase domain (F1 complex), which is composed, among others, of three α subunits (1, 3, 49). Oxidative damage of the α subunit of the mitochondrial ATP-synthase gene promoter causes down-regulation of the protein expression, which leads to reduced ATP synthesis and to nuclear DNA damage of vulnerable genes (27). Oxidative damage to ATP-synthase results in lost of activity (40). Previous studies have also shown significant nitration of the α subunit of ATP-synthase in advanced stages of AD, thus contributing to abnormal function of the respiratory chain (51). Recently, ATP-synthase lipoxidation has been observed in the hippocampus and parietal cortex in cases with mild cognitive impairment neuropathologically verified AD stages III–VI (40). Our results, therefore, do not merely confirmat but rather show for the first time that lipoxidative damage occurs in vulnerable regions from the very early stages of AD, that selective lipoxidation of ATP-synthase is a very early abnormality in AD-related pathology and that this structural modification is associated with a loss of ATPase activity.

Previous studies have shown mitochondrial and energy-related abnormalities in advanced AD. Cytochrome c oxidase (COX), the complex IV of the electron transport chain, expression and activity are impaired in several brain regions in advanced AD (2, 33). In the same line, reduced COX expression, in spite of massive increase of

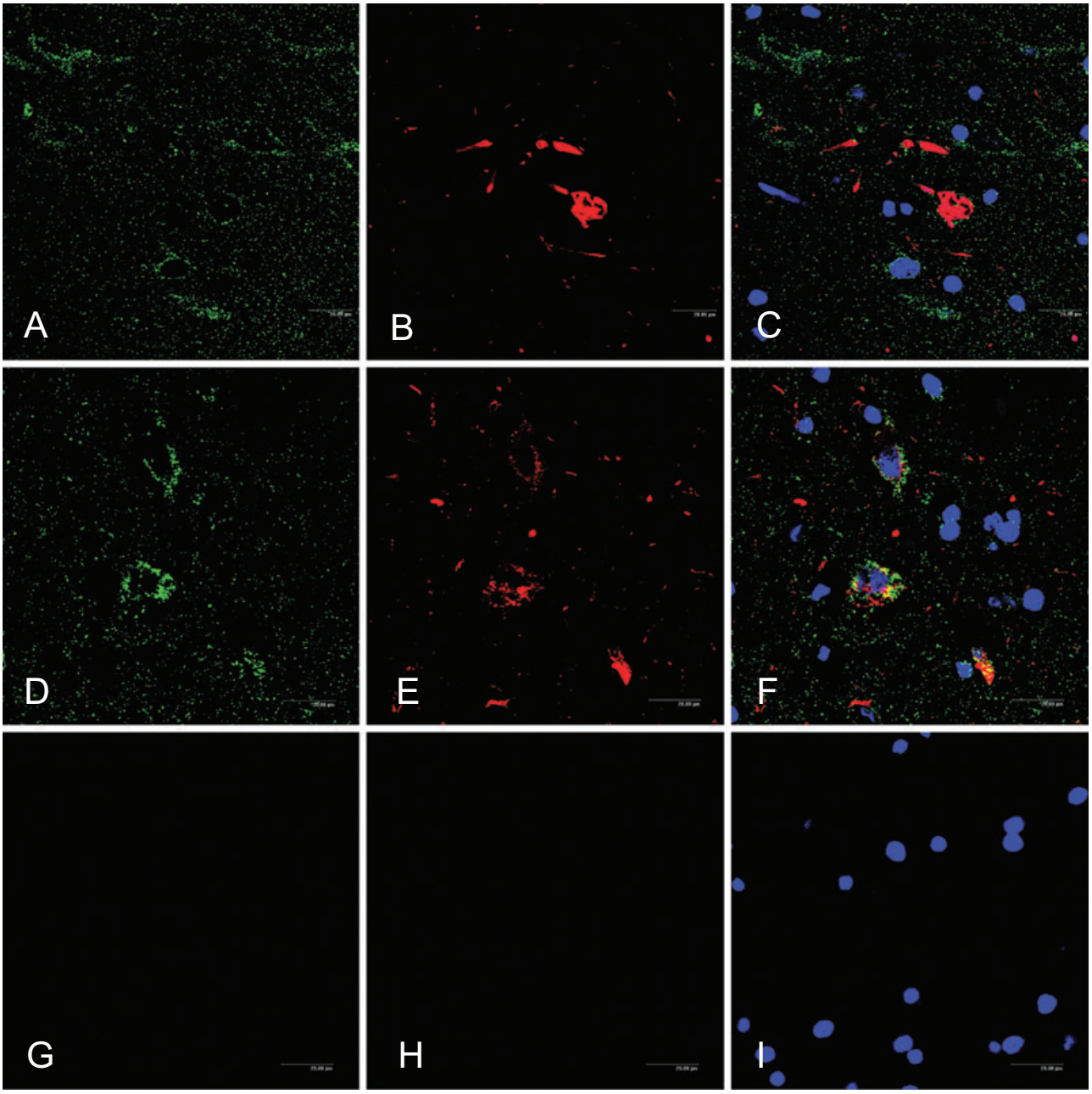

Figure 6. Immunofluorescence and confocal microscopy showing ATP-synthase immunoreactivity (A, D, green) in neurons with tangles (B, red) and pretangles (E, red), as well as in neurons without tau-immunoreactive deposits (A–F), (C, F) merge, (G–I) negative controls incubated without the primary antibodies. Nuclei are visualized in blue. Abbreviation: ATP = ATP-synthase.

aberrant mitochondria, has been recently reported in dystrophic neurites of SPs (38). The α subunit of the ATP-synthase is one of the key targets of oxidative insults in AD brains (40). Decreased α-ketoglutarate dehydrogenase activity, possibly due to the HNE binding, has also been described in parietal and temporal cortices of AD cases (13–15).

Amyloid deposits were present in some but not all AD cases examined in the present study. Therefore, these findings suggest a lack of correlation between β-amyloid deposits and oxidative modification of ATP-synthase α subunit in the entorhinal cortex of AD stage I/II cases analyzed. It is possible that the oxidative damage of the enzyme and the presence of β-amyloid aggregates are two independent events that may co-occur in certain individuals with NFTs restricted to the entorhinal and transentorhinal cortices.

It is not clear whether the present patients with stages I/II of Braak would have progressed to more advanced stages of AD eventually leading to dementia if they had survived. However, considering the proposal of Braak as an instrumental classification, we can

speculate that the onset and then the progression of AD may be the result of the impairment of different cellular pathways whose combination reinforces their effect on cellular damage. In this line, the oxidation of the F1 domain α subunit may impair the activity of the ATP-synthase complex, leading to decreased ATP production and, possibly, to the alteration of the entire electron transport chain function. This could favor, in turn, the overproduction of ROS and the progression of oxidative damage.

In summary, the study shows that the α subunit of the ATP-synthase is targeted for oxidative damage at the very early stages of AD pathology. These results suggest that the possible alteration of the biologic function of this enzyme may be an early and essential step in the pathogenesis of AD. Moreover, our data provide a valuable insight into the important role that oxidative stress plays at the initial stage of AD pathology.

ACKNOWLEDGMENTS

This work was funded by grants from the Spanish Ministry of Health, Instituto de Salud Carlos III FIS PI05/1570, PI05/2214 and PI08/0582, and supported by the European Commission under the Sixth Framework Programme (BrainNet Europe II, LSHM-CT-2004-503039) to IF and in part by I + D grants from the Spanish Ministry of Education and Science (BFU2006-14495/BFI), the Spanish Ministry of Health (ISCIII, Red de Envejecimiento y Fragilidad, RD06/0013/0012), the Generalitat of Catalunya (2005SGR00101) and "La Caixa" Foundation to MPO and RP. We thank Maria Antonia Odena Caballol, David Bellido Español and Eliandre de Oliveira for the proteomics work that was carried out at the Proteomics Platform of Barcelona Science Park, University of Barcelona, a member of ProteoRed network. BT is the recipient of a Beatriu de Pinós fellowship from the Generalitat de Catalunya. We thank T. Yohannan for editorial help. There is no conflict of interest including any financial, personal or other relationships with other people or organizations within the 3 years from the beginning of the work. Brain samples were obtained from the Institute of Neuropathology Brain Bank according to the guidelines and approval of the local Ethics committee.

REFERENCES

1. Abrahams JP, Leslie AG, Lutter R, Walker JE (1994) Structure at 2.8 a resolution of f1-atpase from bovine heart mitochondria. *Nature* **370**:621–628.
2. Bosetti F, Brizzi F, Barogi S, Mancuso M, Siciliano G, Tendi EA *et al* (2002) Cytochrome c oxidase and mitochondrial F1F0-ATPase (ATP synthase) activities in platelets and brain from patients with Alzheimer's disease. *Neurobiol Aging* **23**:371–376.
3. Boyer PD (1997) The ATP synthase—a splendid molecular machine. *Annu Rev Biochem* **66**:717–749.
4. Braak H, Alafuzoff I, Arzberger T, Kretzschmar H, Del Tredici K (2006) Staging of Alzheimer disease-associated neurofibrillary pathology using paraffin sections and immunocytochemistry. *Acta Neuropathol* **112**:389–404.
5. Braak H, Braak E, Peter J, Morrison JH (1999) Temporal sequence of Alzheimer's disease related pathology. In: *Cerebral Cortex*, Vol. 14, *Neurodegenerative and Age-Related Changes in Structure and Function of Cerebral Cortex*, Peters A, Morrison JH (eds), pp. 475–512. Kluwer Academic/Plenum Publishers: New York.
6. Butterfield DA, Gnjec A, Poon HF, Castegna A, Pierce WM, Klein JB, Martins RN (2006) Redox proteomics identification of oxidatively modified brain proteins in inherited Alzheimer's disease: an initial assessment. *J Alzheimers Dis* **10**:391–397.
7. Butterfield DA, Poon HF, St Clair D, Keller JN, Pierce WM, Klein JB, Markesbery WR (2006) Redox proteomics identification of oxidatively modified hippocampal proteins in mild cognitive impairment: insights into the development of Alzheimer's disease. *Neurobiol Dis* **22**:223–232.
8. Butterfield DA, Reed T, Perluigi M, De Marco C, Coccia R, Cini C, Sultana R (2006) Elevated protein-bound levels of the lipid peroxidation product, 4-hydroxy-2-nonenal, in brain from persons with mild cognitive impairment. *Neurosci Lett* **397**:170–173.
9. Davies MJ (2005) The oxidative environment and protein damage. *Biochim Biophys Acta* **703**:93–109.
10. Ding Q, Dimayuga E, Keller JN (2007) Oxidative damage, protein synthesis, and protein degradation in Alzheimer's disease. *Curr Alzheimer Res* **4**:73–79.
11. Duyckaerts C, Dickson DW (2003) Neuropathology of Alzheimer's disease. In: *Neurodegeneration. The Molecular Pathology of Dementia and Movement Disorders*. DW Dickson (ed.), pp. 47–65. ISN Neuropath Press: Basel, Switzerland.
12. Giasson BI, Ischiropoulos H, Lee VM, Trojanowski JQ (2002) The relationship between oxidative/nitrative stress and pathological inclusions in Alzheimer's and Parkinson's diseases. *Free Radic Biol Med* **32**:1264–1275.
13. Gibson GE, Blass JP, Beal MF, Bunik V (2005) The α-ketoglutarate-dehydrogenase complex: a mediator between mitochondria and oxidative stress in neurodegeneration. *Mol Neurobiol* **31**:43–63.
14. Gibson GE, Park LC, Sheu KF, Blass JP, Calingasan NY (2000) The α-ketoglutarate dehydrogenase complex in neurodegeneration. *Neurochem Int* **36**:97–112.
15. Gibson GE, Sheu KF, Blass JP (1998) Abnormalities of mitochondrial enzymes in Alzheimer disease. *J Neural Transm* **105**:855–870.
16. Hatefi Y, Stiggall DL (1978) Preparation and properties of NADH: cytochrome c oxidoreductase (complex I-III). *Methods Enzymol* **53**:5–10.
17. Hütter E, Renner K, Pfister G, Stöckl P, Jansen-Dürr P, Gnaiger E (2004) Senescence-associated changes in respiration and oxidative phosphorylation in primary human fibroblasts. *Biochem J* **380**:919–928.
18. Hyun DH, Lee MH, Halliwell B, Jenner P (2002) Proteasomal dysfunction induced by 4-hydroxy-2,3-trans-nonenal, an end-product of lipid peroxidation: a mechanism contributing to neurodegeneration? *J Neurochem* **83**:360–370.
19. Ingelsson M, Fukumoto H, Newell KL, Growdon JH, Hedley-Whyte ET, Frosch MP *et al* (2004) Early Abeta accumulation and progressive synaptic loss, gliosis, and tangle formation in AD brain. *Neurology* **62**:925–931.
20. Keller JN, Schmitt FA, Scheff SW, Ding Q, Chen Q, Butterfield DA, Markesbery WR (2005) Evidence of increased oxidative damage in subjects with mild cognitive impairment. *Neurology* **64**:1152–1156.
21. Korolainen MA, Goldsteins G, Nyman TA, Alafuzoff I, Koistinaho J, Pirttila T (2006) Oxidative modification of proteins in the frontal cortex of Alzheimer's disease brain. *Neurobiol Aging* **27**:42–53.
22. Kuznetsov AV, Strobl D, Ruttmann E, Königsrainer A, Margreiter R, Gnaiger E (2002) Evaluation of mitochondrial respiratory function in small biopsies of liver. *Anal Biochem* **305**:186–194.
23. Ledesma MD, Bonay P, Colaco C, Avila J (1994) Analysis of microtubule-associated protein tau glycation in paired helical filaments. *J Biol Chem* **269**:21614–21619.

24. Lovell MA, Ehmann WD, Mattson MP, Markesbery WR (1997) Elevated 4-hydroxynonenal in ventricular fluid in Alzheimer's disease. *Neurobiol Aging* **18**:457–461.
25. Lovell MA, Markesbery WR (2007) Oxidative DNA damage in mild cognitive impairment and late-stage Alzheimer's disease. *Nucleic Acids Res* **35**:7497–7504.
26. Lovell MA, Markesbery WR (2008) Oxidatively modified RNA in mild cognitive impairment. *Neurobiol Dis* **29**:169–175.
27. Lu T, Pan Y, Kao SY, Li C, Kohane I, Chan J, Yankner BA (2004) Gene regulation and DNA damage in the ageing human brain. *Nature* **429**:883–891.
28. Magaki S, Raghavan R, Mueller C, Oberg KC, Vinters HV, Kirsch WM (2007) Iron, copper, and iron regulatory protein 2 in Alzheimer's disease and related dementias. *Neurosci Lett* **418**:72–76.
29. Mariani E, Monastero R, Mecocci P (2007) Mild cognitive impairment: a systematic review. *J Alzheimers Dis* **12**:23–35.
30. Mark RJ, Fuson KS, May PC (1999) Characterization of 8-epiprostaglandin F2α as a marker of amyloid beta-peptide-induced oxidative damage. *J Neurochem* **72**:1146–1153.
31. Mark RJ, Lovell MA, Markesbery WR, Uchida K, Mattson MP (1997) A role for 4-hydroxynonenal, an aldehydic product of lipid peroxidation, in disruption of ion homeostasis and neuronal death induced by amyloid beta-peptide. *J Neurochem* **68**:255–264.
32. Markesbery WR (1997) Oxidative stress hypothesis in Alzheimer's disease. *Free Radic Biol Med* **23**:134–147.
33. Maurer I, Zierz S, Moller HJ (2000) A selective defect of cytochrome c oxidase is present in brain of Alzheimer disease patients. *Neurobiol Aging* **21**:455–462.
34. Naudí A, Caro P, Jové M, Gómez J, Boada J, Ayala V *et al* (2007) Methionine restriction decreases endogenous oxidative molecular damage and increases mitochondrial biogenesis and uncoupling protein 4 in rat brain. *Rejuvenation Res* **10**:473–484.
35. Nunomura A, Castellani RJ, Zhu X, Moreira PI, Perry G, Smith MA (2006) Involvement of oxidative stress in Alzheimer disease. *J Neuropathol Exp Neurol* **65**:631–641.
36. Nunomura A, Perry G, Aliev G, Hirai K, Takeda A, Balraj EK *et al* (2001) Oxidative damage is the earliest event in Alzheimer disease. *J Neuropathol Exp Neurol* **60**:759–767.
37. Pamplona R, Dalfo E, Ayala V, Bellmunt MJ, Prat J, Ferrer I, Portero-Otin M (2005) Proteins in human brain cortex are modified by oxidation, glycoxidation, and lipoxidation. Effects of Alzheimer disease and identification of lipoxidation targets. *J Biol Chem* **280**:21522–21530.
38. Pere-Gracia E, Torrejón-Escribano B, Ferrer I (2008) Dystrophic neurites of senile plaques in Alzheimer's disease are deficient in cytochrome c oxidase. *Acta Neuropathol* **116**:409–418.
39. Petersen RC (2000) Mild cognitive impairment: transition between aging and Alzheimer's disease. *Neurology* **15**:93–101.
40. Reed T, Perluigi M, Sultana R, Pierce WM, Klein JB, Turner DM *et al* (2008) Redox proteomic identification of 4-hydroxy-2-nonenal-modified brain proteins in amnestic mild cognitive impairment: insights into the role of lipid peroxidation in the progression and pathogenesis of Alzheimer's disease. *Neurobiol Dis* **30**:107–120.
41. Renner K, Amberger A, Konwalinka G, Kofler R, Gnaiger E (2003) Changes of mitochondrial respiration, mitochondrial content and cell size after induction of apoptosis in leukemia cells. *Biochim Biophys Acta* **1642**:115–123.
42. Saito Y, Murayama S (2007) Neuropathology of mild cognitive impairment. *Neuropathology* **27**:578–584.
43. Sayre LM, Smith MA, Perry G (2001) Chemistry and biochemistry of oxidative stress in neurodegenerative disease. *Curr Med Chem* **8**:721–738.
44. Srere PA (1969) Citrate synthase. *Methods Enzymol* **13**:3–11.
45. Smith MA, Harris PL, Sayre LM, Perry G (1997) Iron accumulation in Alzheimer disease is a source of redox-generated free radicals. *Proc Natl Acad Sci U S A* **94**:9866–9868.
46. Smith MA, Rottkamp CA, Nunomura A, Raina AK, Perry G (2000) Oxidative stress in Alzheimer's disease. *Biochim Biophys Acta* **1502**:139–144.
47. Smith MA, Taneda S, Richey PL, Miyata S, Yan SD, Stern D *et al* (1994) Advanced Maillard reaction end products are associated with Alzheimer disease pathology. *Proc Natl Acad Sci U S A* **91**:5710–5714.
48. Stadtman ER (1992) Protein oxidation and aging. *Science* **257**:1220–1224.
49. Stock D, Gibbons C, Arechaga I, Leslie AG, Walker JE (2000) The rotary mechanism of ATP synthase. *Curr Opin Struct Biol* **10**:672–679.
50. Sultana R, Boyd-Kimball D, Poon HF, Cai J, Pierce WM, Klein JB *et al* (2006) Redox proteomics identification of oxidized proteins in Alzheimer's disease hippocampus and cerebellum: an approach to understand pathological and biochemical alterations in AD. *Neurobiol Aging* **27**:1564–1576.
51. Sultana R, Poon HF, Cai J, Pierce WM, Merchant M, Klein JB *et al* (2006) Identification of nitrated proteins in Alzheimer's disease brain using a redox proteomics approach. *Neurobiol Dis* **22**:76–87.
52. Sultana R, Reed T, Perluigi M, Coccia R, Pierce WM, Butterfield DA (2007) Proteomic identification of nitrated brain proteins in amnesic mild cognitive impairment: a regional study. *J Cell Mol Med* **11**:839–851.
53. Uchida K (2003) 4-Hydroxy-2-nonenal: a product and mediator of oxidative stress. *Prog Lipid Res* **42**:318–343.
54. Williams TI, Lynn BC, Markesbery WR, Lovell MA (2006) Increased levels of 4-hydroxynonenal and acrolein, neurotoxic markers of lipid peroxidation, in the brain in mild cognitive impairment and early Alzheimer's disease. *Neurobiol Aging* **27**:1094–1099.
55. Wyss-Coray T (2006) Inflammation in Alzheimer disease: driving force, bystander or beneficial response? *Nat Med* **12**:1005–1015.
56. Yan SD, Chen X, Schmidt AM, Brett J, Godman G, Zou YS *et al* (1994) Glycated tau protein in Alzheimer disease: a mechanism for induction of oxidant stress. *Proc Natl Acad Sci U S A* **91**:7787–7791.